Eur. J. Mineral.
1990, **2**, 89-102

Isotopic dating of adularia-bearing epigenetic mineralizations : I. Saar-Nahe region/Southwest Germany

DIETER F. MERTZ [1,3], HANS J. LIPPOLT [1] and GERHARD MÜLLER [2]

[1] Laboratorium für Geochronologie der Universität, Im Neuenheimer Feld 234, D-6900 Heidelberg

[2] Im Flürchen 7, D-6601 Saarbrücken-Scheidt

Abstract : Isotopic age determinations ($^{40}Ar/^{39}Ar$, Rb/Sr) on hydrothermally formed K-feldspars (adularia) from epigenetic vein mineralizations in the Saar-Nahe region (SW Germany) yielded age values of 224 Ma and 219 Ma. This places mineralizing activities in this region in the Upper Triassic. The geological significance of the isotopic data is assured by age concordances between a) the Rb/Sr and K/Ar systems, b) petrographically different adularia types and c) adularia from different locations. According to chemical and X-ray structural investigations, the adularia are pure K-feldspars with Or contents > 98 mol.% with a relatively high degree of Al,Si disorder. Due to the paragenetic position of the adularia within the sequence of the Saar-Nahe mineralizations as well as to the corresponding experimentally determined time marks, a considerable number of these mineralizations can be attributed to a syn- to post-Triassic age. A genetic relationship to the Permian magmatism of the Saar-Nahe region does not exist for these mineralizations in the sense of a post-magmatic sequence. This conclusion is supported by the $^{87}Sr/^{86}Sr$ variation of paragenetic calcites of 0.7103 ± 0.0006 which is significantly higher than the Sr initial ratios of the Permian magmatic rocks. The mineralizing events confirm an Upper Triassic super-regional hydrothermal phase whose existence has already been established for Western and Southern Europe and can now be extended to Central Europe.

Key-words : adularia, $^{40}Ar/^{39}Ar$ dating, Rb/Sr dating, mineralization, Southwest Germany.

1. Introduction

Adularia are hydrothermally formed K-feldspars and are characterized morphologically – in contrast to other K-feldspar types – by the dominance of (110) and ($\bar{1}01$) faces (*e.g.* Franke and Ghobarkar, 1982). Munhá *et al.* (1980) determined, based on oxygen isotopic fractionation, crystallization temperatures of adularia in sea-floor rhyolites to be less than 140 °C. The crystallization temperatures of recent adularia in geothermal fields are below 265 °C (Steiner, 1968 ; 1970). Adularia are found in related geological environments in parageneses of economically important mineralizations, *e.g.,* in the inner zones of porphyry Cu deposits (*e.g.* Rose, 1970), in vein-like U deposits (*e.g.* Rich *et al.,* 1977), in Au-bearing quartz veins (*e.g.* Silberman *et al.,* 1972), in sub-volcanic Au-Ag vein deposits (*e.g.* Buchanan, 1981) or in baryte-fluorite vein mineralizations (*e.g.* Ziehr, 1967). Neogenic low-temperature K-feldspars are also known to exist in sedimentary (*e.g.* Kastner and Siever, 1979), magmatic and metamorphic environments (*e.g.* Mensing and Faure, 1983).

Particularly in hydrothermal mineralizations, adularia is of substantial interest with respect to the genesis of ores and gangues. As a K and Rb-bearing mineral, it may serve as a possible isotopic geochronometer for K/Ar and Rb/Sr

[3] Now at Geologisch-Paläontologisches Institut der Universität Kiel.

0935-1221/90/0002-0089 $ 3.50

dating. The paragenetic position of adularia in epigenetic deposits is often well definable within the polycyclic sequences of tectonics and mineralization (*e.g.* Badham, 1975 ; Mertz *et al.,* 1989a). This permits the attribution of acquired isotopic age data to specific mineralizing events. Thus, it is possible to recognize causal mechanisms between the general geological evolution and the genesis of mineralizations. With the exception of a few minerals (*e.g.* Silberman and Ashley, 1970), other gangue and ore minerals are not suitable for isotopic K/Ar and Rb/Sr dating, as the radioactive nuclides ^{40}K and ^{87}Rb are not present in sufficient quantities.

The concordance of Rb/Sr (Lippolt *et al.,* 1985), K/Ar (Brockamp and Zuther, 1985) and $^{40}Ar/^{39}Ar$ ages (Mertz, 1987) of adularia of the same paragenesis from the Wölsendorf ore district (South Germany), indicates that hydrothermally formed K-feldspar may supply geologically significant age data. However, it is known that adularia are often susceptible to isotopic disturbance, which is evident in discordant K/Ar and Rb/Sr ages (Bass and Ferrara, 1969 ; Mertz *et al.,* 1989a). These disturbances might be caused by Ar losses due to later hydrothermal (Kämpf and Pilot, 1981) or metamorphic (Bass and Ferrara, 1969) overprints or by changes of the structural state of the K-feldspars (Halliday and Mitchell, 1976). On the other hand, adularia are also known as reservoirs of excess argon (Joseph *et al.,* 1973 ; Purdy and Stalder, 1973 ; Hess, 1985). The results of the studies cited show that the application of adularia as isotopic chronometer in hydrothermal environment leaves a number of questions without a satisfying final answer.

Isotopic K/Ar or $^{40}Ar/^{39}Ar$ and Rb/Sr datings were carried out on adularia from epigenetic vein mineralizations in SW Germany (Saar-Nahe area, Odenwald, Pfälzerwald and Schwarzwald). The main objectives of these investigations were 1) to work out the argon isotope systematics of adularia and 2) to explain geological aspects of the genesis of the mineralizations, in particular their temporal positions as well as causal correlations to the overall geotectonic evolution. The adularia analyzed in this study, which have been described by Müller (1975), are from mineralizations in the Saar-Nahe region.

2. Geological setting

The investigated mineralizations are located

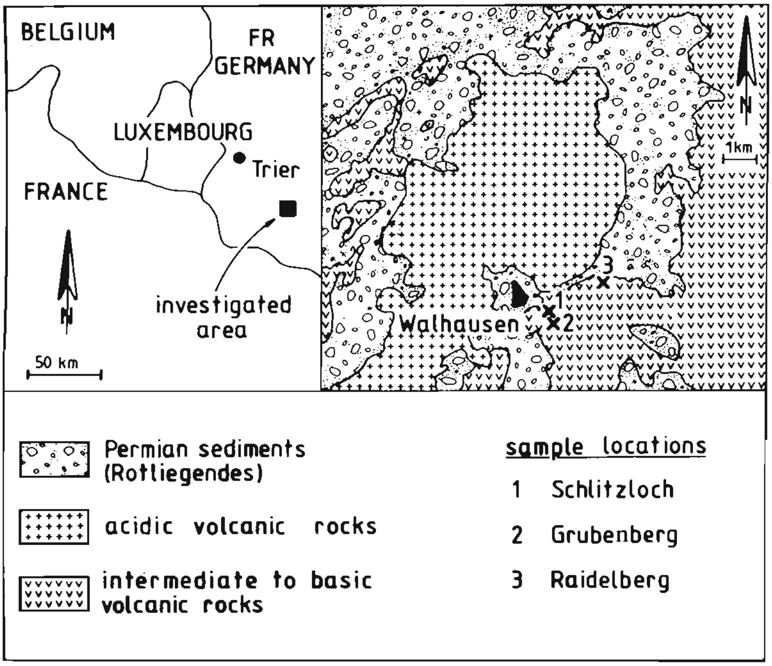

Fig. 1. Geographical and geological positions of the investigated mineralizations.

in the Saar-Nahe region (SW Germany) about 50 km SE of Trier, 1 to 2 km W of the village Walhausen (Fig. 1). The locations Schlitzloch, Grubenberg and Raidelberg represent the sampling points. The geological map of the "Saar-Nahe Bergland" 1:100000 (Dreyer *et al.*, 1983) displays Permian intermediate to basic effusive rocks and acid magmatic rocks in the area of the mineralizations. This magma production is part of a phase of intensive volcanic activity which accompanied the formation of intramontanous basins in various parts of Europe after the Hercynian orogen. In the Saar-Nahe basin, tuffs and volcanic rocks were supplied during the Rotliegendes. Together with clastic-terrestrial sediments they form the so-called "Grenzlager", a lithological unit at the basis of the Upper Rotliegendes (*e.g.* Falke, 1959 ; Bambauer, 1960 ; Jung, 1970). K/Ar and $^{40}Ar/^{39}Ar$ systematics yielded an age range of 295-300 Ma for biotites from rhyolites and tuffs of the "Grenzlager" (Lippolt and Hess, 1983). A Rb/Sr isochron (biotite and apatite, n = 27) gave an age of 291 ± 1 Ma (Lippolt *et al.*, 1989).

3. Mineralization and parageneses

The mineralizations investigated are vein-like Pb-Cu mineralizations, related to tectonically fractured zones. The paragenetic succession is outlined in Fig. 2. Müller (1983 ; 1988) makes a distinction between an older Saxonian and a younger Saxonian mineralization period with an obvious hiatus. The succession of the older mineralization period, from old to young, is saponite, adularia and quartz, followed by the ores galena, tetrahedrite and chalcopyrite I. In the younger mineralization period, the ores digenite, chalcocite and chalcopyrite II were deposited. Calcite is ubiquitous. According to Müller (1983 ; 1988), this succession in principle may be attributed to a large-scale existing paragenetic succession, which is observed in various parts of the whole Saar-Nahe-Pfalz region. The isotopic dating of the adularia supplies an older time mark for the ores of the older and the younger mineralization periods due to its defined position within the paragenetic succession. The large-scale consistence of paragenetic relations makes this time mark not only of local importance for the Walhausen mineralization. It is also significant for the metallogenesis in the super-regional context.

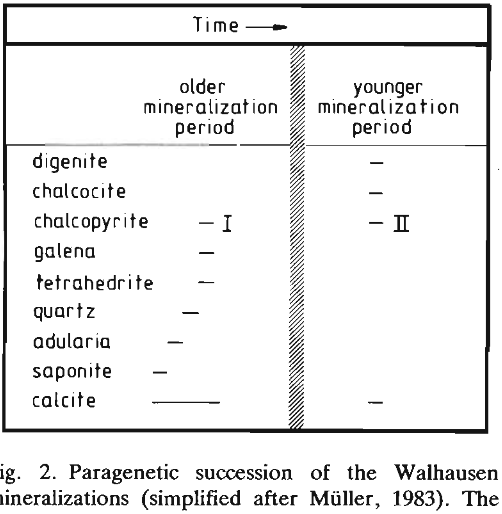

Fig. 2. Paragenetic succession of the Walhausen mineralizations (simplified after Müller, 1983). The hatching indicates a (non-defined) hiatus between an older and a younger mineralization period.

4. Description of the dated adularia

4.1. Petrography

Thin-section investigations show that the host rocks of the mineralizations are tectonically overprinted andesitic rocks with alteration phenomena of various intensities. The tectonic stress is evident in numerous fractures of the plagioclase xenocrysts. Most of the fractures were healed by a probably syntectonic iron ore phase. Evident alterations are the replacement of mafics (probably hornblende) by ore and Mg,Fe sheet silicates, as well as the crystallization of authigenic K-feldspars which in turn may be affected by ore impregnations or light micatizations.

Principally, the authigenic K-feldspars occur in three different types : Type A is an idiomorphic to hypidiomorphic crystal with adularia habit in vesicular spaces (Fig. 3) and in joints. The K-feldspars are defined in the paragenetic sequence of the mineralization. Type B consists of xenomorphic poly-aggregates which replace dispersely the groundmass of the andesitic rocks (Fig. 4). Type C is a K-feldspar which replaces the plagioclase xenocrysts (Fig. 5). Type B and C of K-feldspars indicate that the andesitic host rock of the mineralizations has

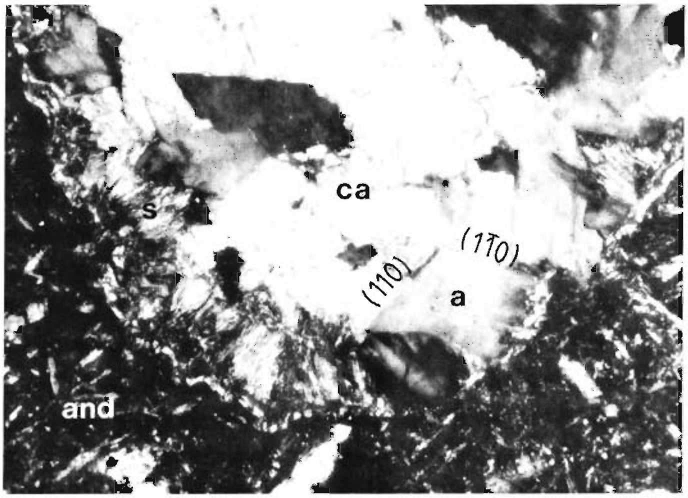

Fig. 3. Thin section (+N, width of photograph approx. 1.1 mm) of neogenic K-feldspar of type A : idiomorphic to hypidiomorphic crystals with adularia habit. The adularia (a) occur in vesicles in andesitic rocks (and), some of them have grown on fibrous sheet silicates (s). The marked adularia crystal shows a cut approx. ⊥ [001] with well-developped (110) and (1$\bar{1}$0) faces.

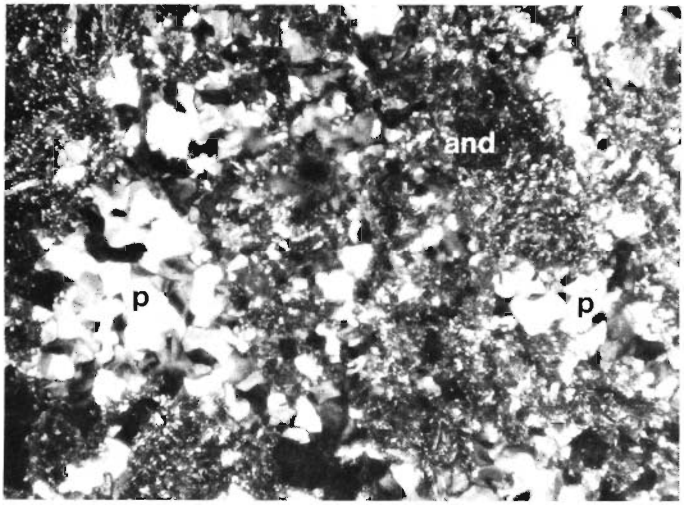

Fig. 4. Thin section (+N, width of photograph approx. 2.7 mm) of neogenic K-feldspar of type B : xenomorphic poly-aggregates (p) dispersely replace ground mass of andesitic rocks (and).

been affected by a K-metasomatosis. A correlation between the genesis of adularia and the K-metasomatic overprint of the wall rocks is assumed to be very likely. Similar phenomena of K-feldspar displacements are reported by Steiner (1970) on post-Miocene rhyolitic rocks within a recent geothermal field. Cathodoluminescence investigations on K-feldspars of type A show that these adularia display a zoned structure (Fig. 6), documenting a quasi phase-like growth of adularia.

4.2. Measured samples

Conventional mineral-separation methods (crushing, sieving, magnetic separation, density

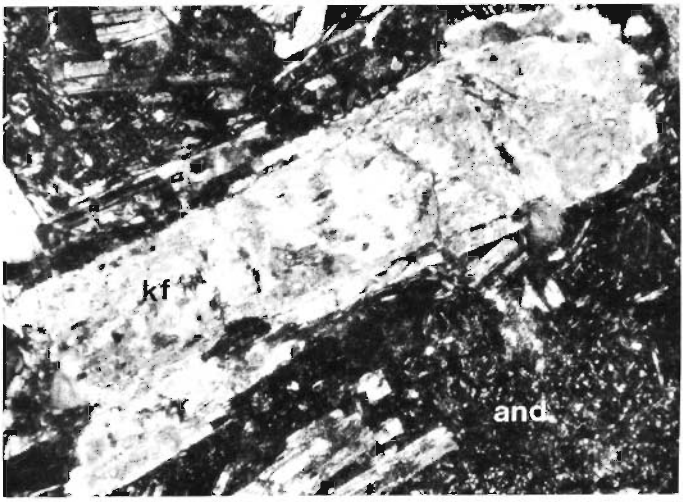

Fig. 5. This section (+N, width of photograph approx. 2.7 mm) of neogenic K-feldspar of type C : replacements of plagioclase xenocrysts in andesitic rocks (and) with typical spotty extinction of the K-feldspar.

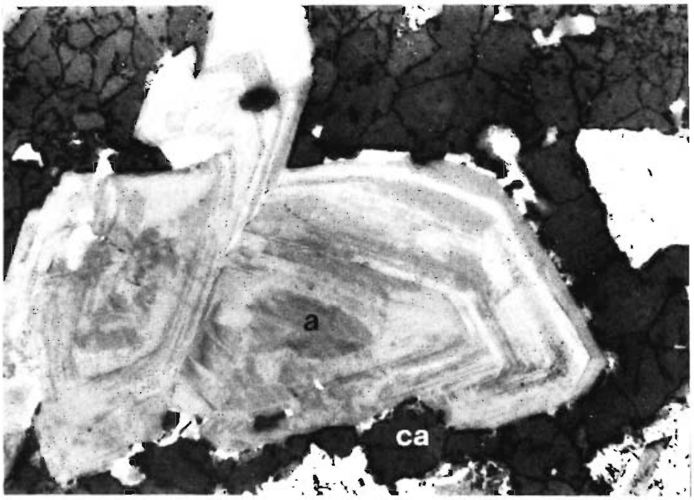

Fig. 6. Cathodoluminescence photograph (width of photograph about 0.4 mm) of neogenic K-feldspar of type A : the adularia crystals (a) show a clear zoned structure (original luminescence colour : dark-red). At the rims, a replacement of adularia by calcite (ca) (original luminescence colour : lilac) takes place.

separation, hand-picking) were performed. K-feldspar samples from the locations Schlitzloch, Grubenberg and Raidelberg for $^{40}Ar/^{39}Ar$ and Rb/Sr measurements, as well as calcites from the locations Schlitzloch and Grubenberg for $^{87}Sr/^{86}Sr$ measurements were prepared. The compositions of the K-feldspar separates were checked using grain thin-sections. Table 1 lists the petrographic characteristics of the samples. The separates Grubenberg 01 and Raidelberg 01 are colourless-milky adularia, Grubenberg 02 represents colourless-clear adularia, Schlitzloch 01 are milky and clear adularia with slight sheet-silicate contamination. Sample Grubenberg 03 represents adularia overprinted by slight to intensive ore impregnations. All measured samples are exclusively K-feldspars of type A, comprised of different adularia

Table 1. Petrographic description of the measured K-feldspar separates.

Sample	Relative composition	Colour/transparency
Grubenberg 01*	>97% Type A	colourless-milky
Grubenberg 02*	>97% Type A	colourless-clear
Grubenberg 03**	≈90% Type A	colourless to reddish
	≈10% ore (weak to intensive impregnation)	
Raidelberg 01*	>97% Type A	colourless-milky
Raidelberg 02*	≈60% Type A	colourless to sligthly reddish,
	≈40% Type B	very weak ore impregnation
Schlitzloch 01*	≈95% Type A	colourless, milky to clear
	≈ 5% sheet silicates	
Schlitzloch 02*	≈70% Type A	colourless-milky
	≈10% Type B	to reddish
	≈20% ore (weak to intensive impregnation)	

* separate for $^{40}Ar/^{39}Ar$ analysis
** separate for Rb/Sr analysis

populations (milky, colourless, etc.). Raidelberg 02 and Schlitzloch 02 are mixed separates which contain K-feldspars of type A and B and display ore impregnations of various intensities.

For the strontium isotopic measurements, calcites were extracted from small veins (Schlitzloch : WS ca 01-a to WS ca 01-c, Grubenberg : WG ca 01) and from vesicles (*cf.* Fig. 3) in andesitic host rocks (Schlitzloch : WS ca 02, Grubenberg : WG ca 02).

4.3. Chemical composition and X-ray structure

In order to characterize the adularia chemically and structurally and to recognize possible correlations between isotopic behavior and mineralogical state, microprobe and X-ray structural analyses were carried out on selected samples. Table 2 presents the chemical composition of the adularia Schlitzloch 01 and 02 together with reference data on adularia from two other Central European vein mineralizations. The adularia analyzed are K-feldspars of type A, whereas Schlitzloch 02, in contrast to separate 01, displays intensive iron-ore impregnations. Both samples show nearly the same composition (*cf.* Table 2). The SiO_2, Al_2O_3 and K_2O contents are in good concordance with the reference data. The CaO and Na_2O contents deviate. For the Schlitzloch adularia, the albite and anorthite components are below the litera-

Table 2. Chemical compositions of the adularia samples Schlitzloch 01 and Schlitzloch 02 (microprobe analyses) as well as reference analyses of adularia from other Central European vein deposits.

Sample:		Schlitz-loch 01	Schlitz-loch 02	Wölsen-dorf[1)]	Schmiede-berg[2)]
Wt.-%	SiO_2	64.36	64.18	64.07	64.63
	TiO_2	0.05	b.d.	n.d.	n.d.
	Al_2O_3	18.76	18.41	18.80	18.62
	FeO	0.01*	0.85*	0.47**	n.d.
	MgO	n.d.	n.d.	0.20	n.d.
	MnO	b.d.	b.d.	n.d.	n.d.
	CaO	0.01	b.d.	0.53	0.45
	BaO	n.d.	n.d.	b.d.	n.d.
	Na_2O	0.04	0.11	0.34	1.11
	K_2O	16.29	15.88	15.43	15.39
	Total	99.52	99.43	99.84	100.20
Numbers of ions on the basis of 32 O					
	Si	11.899	11.951	11.827	11.979
	Al	4.153	4.040	4.091	4.046
	Σ Z	16.052	15.991	15.918	15.963
	Ti	0.007			
	Fe	0.001	0.132	0.064	
	Mg			0.055	
	Ca	0.001		0.105	0.089
	Na	0.015	0.040	0.122	0.397
	K	3.903	3.771	3.634	3.620
	Σ X	3.928	3.944	3.980	4.106
Mol-%	Or	99.59	98.95	94.12	88.16
	Ab	0.38	1.05	3.16	9.67
	An	0.03		2.72	2.17

b.d.: below detection limit
n.d.: not determined
1) Riederer (1966)
2) Hintze (1897)
* total iron as FeO
** total iron as Fe_2O_3

ture values by approximate factors of 25 and 100, respectively. The relatively high FeO contents of about 0.9 wt.% of adularia Schlitzloch 02 may be assigned to the ore impregnations of the feldspar. Generally, the Schlitzloch adularia are very pure K-feldspars with Or contents > 98.9 mol.%. The reference adularia show significant lower Or contents of about 94 and 88 mol.%, respectively.

X-ray structure analyses of the adularia Raidelberg 01, Schlitzloch 01 and 02, a sanidine standard (Volkesfeld/Eifel, FRG) and of a microcline standard (Gundlebo/Sweden) were carried out using the Guinier technique. The data processing was done photometrically. The three adularia show analogous positions and intensities of diffraction maxima, which are similar to the diffraction pattern of the sanidine standard. A splitting into the line pairs ($1\bar{3}0$) and (130) (MacKenzie, 1954) or ($1\bar{3}1$) and (131) (Goldsmith and Laves, 1954a ; 1954b), which is characteristic for the development of triclinic compounds, is not found in the adularia. However, the (130) and (131) diffraction maxima of the adularia are more widely spread compared to those of the sanidine standard. This is supposed to be due to a weak development of domains with Al,Si ordering tendencies. Taken as a whole, the adularia are to be regarded as radiographically monoclinic K-feldspars with a relatively high state of Al,Si disorder.

5. Isotopic analyses and results

Rb/Sr and K/Ar dating methods were applied, the latter using the $^{40}Ar/^{39}Ar$ technique. Rb and Sr concentrations and isotope compositions were determined using a Finnigan solid-source mass spectrometer MAT 261 with computerized data acquisition. The analysis of the adularia sample Grubenberg 03 yielded a Sr concentration of 6.3 ppm, a Rb concentration of 63 ppm and a $^{87}Sr/^{86}Sr$ ratio of 0.8019 ± 0.0001 (Table 3). Sr ratios of the paragenetic calcites range from 0.7097 to 0.7109 (Table 4). Assuming this $^{87}Sr/^{86}Sr$ variation to be the initial value, a Rb/Sr age of 220.4 ± 4.8 Ma is calculated for the adularia (λ $^{87}Rb = 1.42 \cdot 10^{-11}$ a^{-1}). In order to demonstrate the significance of our data, accompanying concentration and isotope measurements on NBS standards potassium feldspar 607 and $SrCO_3$ 987 were performed. The results of our standard analyses agree with the certified values within analytical errors. Therefore the analytical data are considered to be significant. The exact data of our standard measurements have been discussed by Mertz (1987).

For $^{40}Ar/^{39}Ar$ dating the adularia samples were wrapped in aluminium foil and irradiated (dose approx. $1.5 \cdot 10^{17}$ and $5 \cdot 10^{17}$) in cadmium-mantled evacuated quartz ampoules in a reactor of the Nuclear Research Centre Jülich (FRG). Each adularia sample was positioned between two standards. The irradiation gradients between two standards ranged from 1 to 8 %. Stepwise heating technique was applied. Ar extraction was done in an inductively heated molybdenum crucible or in a resistance-heated low blank vacuum apparatus modified after Staudacher *et al.* (1978). Ar blanks at 1h/1600°C were approx. $2 \cdot 10^{-8}$ or $4 \cdot 10^{-9}$ cm^3 STP for the inductively heated crucible or the resistance-heated apparatus, respectively, and

Table 3. Rb and Sr concentration and isotope measurements on the adularia sample Grubenberg 03.

Rb [ppm]	Sr [ppm]	$^{87}Rb/^{86}Sr$	$^{87}Sr/^{86}Sr_t$	$^{87}Sr/^{86}Sr_i$	Age [Ma]
63.1 ± 0.2	6.26 ±0.02	29.22 ± 0.09	0.80188 ±0.00008	0.7103 ±0.0006	220.4 ± 4.8

The age of the adularia is 220.4 ± 4.8 Ma, calculated with an initial Sr ratio of 0.7103 ± 0.0006, corresponding to the $^{87}Sr/^{86}Sr$ spectrum of paragenetic calcites (Analytical errors : $1-\sigma$).

Table 4. $^{87}Sr/^{86}Sr$ ratios of various calcites from the Walhausen mineralizations Schlitzloch (WS) and Grubenberg (WG).

Sample	$^{87}Sr/^{86}Sr \pm 1\text{-}\sigma$
ca WS 01-a	0.70989 ± 0.00008
ca WS 01-b	0.70971 ± 0.00002
ca WS 01-c	0.70987 ± 0.00003
ca WS 02	0.70994 ± 0.00002
ca WG 01	0.71088 ± 0.00002
ca WG 02	0.71079 ± 0.00005

better for lower temperatures. The isotopic compositions were measured on a Finnigan gas source mass spectrometer MAT-GD 150 in static mode. Muscovite of the Bärhalde Granite served as working standard ($t_{integrated}$: 326.2 ± 2.0 Ma ; Rittmann, 1984), which has been calibrated against the international hornblende standard MMhb−1 (Alexander *et al.,* 1978). The age calculation is based on the constants recommended by Steiger and Jäger (1977). Table 5 lists the $^{40}Ar/^{39}Ar$ age results of the adularia. The Grubenberg samples 01 and 02 yield integrated ages of 225.0 ± 1.1 Ma and 225.4 ± 1.2 Ma, the Raidelberg samples 01 and 02 yield 218.0 ± 1.3 Ma and 211.9 ± 1.4 Ma, whereas the Schlitzloch samples 01 and 02 yield 220.2 ± 1.3 Ma and 214.1 ± 1.2 Ma (Analytical errors of integrated ages and step age values do not contain monitor uncertainties). The plateau ages are 226.3 ± 3.0 Ma and 226.2 ± 3.5 Ma for the Grubenberg samples 01 and 02, 219.0 ± 2.7 Ma and 218.9 ± 2.8 Ma for the Raidelberg samples 01 and 02, as well as 222.2 ± 3.1 Ma and 214.7 ± 2.4 Ma for the Schlitzloch samples 01 and 02 (Analytical errors of plateau ages contain monitor uncertainties). Fig. 7 displays the degassing spectra.

6. Discussion of the analytical results

All adularia samples show relatively undisturbed $^{40}Ar/^{39}Ar$ degassing spectra with plateau areas each > 70 % of the total ^{39}Ar degassing. The degassing steps in the low-temperature range each display apparent ages considerably younger than the plateau areas. This may be caused by slight Ar losses. Therefore, the plateau ages are considered to be of higher significance than the integrated ages.

For the location Grubenberg, concordant $^{40}Ar/^{39}Ar$ plateau and Rb/Sr ages were obtained on different adularia populations. This concordance, both with independent isotopic systems and with petrographically different populations, indicates the geological significance of these isotopic ages. Considering the overlapping of the analytical errors of $^{40}Ar/^{39}Ar$ and Rb/Sr ages, a hydrothermal event at 224 Ma is manifested, which is interpreted to be the crystallization age of the adularia of the location Grubenberg.

The adularia samples of the location Raidelberg display concordant $^{40}Ar/^{39}Ar$ plateau ages which are lower by about 4 Ma when compared with the Grubenberg data. This hiatus is not attributed to disturbances of the isotopic system by Ar losses of the Raidelberg adularia, but it is caused by the crystallization of two distinct adularia generations at the locations Grubenberg and Raidelberg. This is indicated by the following : a) The Raidelberg adularia has, like the Grubenberg adularia, a relatively undisturbed degassing spectrum with a clearly developed age plateau. b) The X-ray structure investigations show that the sample Raidelberg 01 is a radiographically monoclinic adularia with a relatively high degree of Al,Si disorder. Ar losses like those seen by Halliday and Mitchell (1976) due to the formation of triclinic compounds, therefore, have to be regarded as rather unlikely. c) Ar losses, caused by secondary overprints such as sericitization or ore impregnation, can be ruled out based on microscopic observations. d) Ar vacuum-diffusion analyses on the sample Raidelberg 01 yielded an activation energy for ^{39}Ar of 134 ± 7 kJ/mol (Mertz *et al.,* 1989b). This value corresponds to the range of activation energies for volcanic high sanidines (personal communication Hess and Lippolt, 1989), which are to be regarded as excellent K/Ar chronometers (*e.g.* Hess and Lippolt, 1986). By analogy, this may also apply to the Raidelberg adularia. e) the samples Raidelberg 01 and 02 display different compositions of adularia types (*cf.* Table 1) with concordant K/Ar age data. The concordance of the isotopic ages of petrographically different samples suggests a very low probability of disturbance of the isotopic system. A crystallization age of 219 Ma is therefore assumed for the Raidelberg adularia.

The sample Schlitzloch 01 shows a $^{40}Ar/^{39}Ar$ plateau age which, whithin analytical errors, agrees with the age of Grubenberg and Raidelberg adularia generations. Thus, this age range is confirmed by adularia from a third location. The plateau age of the sample Schlitzloch 02, however, is significantly lower, amounting to about 215 Ma. Since the samples Schlitzloch 01 and 02 are of very similar X-ray structure, the younger age of sample 02 probably cannot be attributed to Ar losses due to a higher degree of Al,Si ordering. Microscopic investigations show that part of the adularia Schlitzloch 02 are intensively impregnated by iron ore, either dispersely or in the shape of

Table 5. Results of $^{40}Ar/^{39}Ar$ incremental heating measurements on adularia samples from the Walhausen mineralizations (Analytical errors : 1−σ).

Temperature [°C]	Time [min]	^{36}Ar	^{39}Ar [$*10^{-9}cm^3STP$]	$^{40}Ar_{total}$	$^{40}Ar_{rad}/^{39}Ar$	Age [Ma]
Sample: Grubenberg 01						$J = 4.290*10^{-3}$
770	45	0.379±0.026	33.39 ±0.11	1008 ± 2	26.83±0.25	196.5± 1.8
860	65	0.161±0.001	131.4 ±0.3	4106 ± 8	30.86±0.10	224.3± 0.7
920	65	0.157±0.017	119.5 ±0.2	3753 ± 8	31.01±0.09	225.3± 0.6
940	65	0.199±0.027	141.6 ±0.4	4457 ±11	31.06±0.14	225.7± 0.9
960	65	0.197±0.010	173.0 ±0.4	5468 ±11	31.26±0.11	227.0± 0.7
1020	65	0.141±0.023	164.6 ±0.4	5204 ±12	31.35±0.12	227.6± 0.8
1060	65	0.080±0.001	96.10 ±0.15	3033 ± 7	31.30±0.08	227.3± 0.6
1100	65	0.145±0.001	123.1 ±0.1	3875 ±10	31.11±0.09	226.0± 0.6
1130	65	0.151±0.038	215.9 ±0.5	6735 ±51	30.97±0.26	225.1± 1.7
1190	65	0.454±0.031	255.9 ±0.7	8116 ±42	31.17±0.19	226.5± 1.3
1220	65	0.286±0.024	158.2 ±0.4	5081 ±11	31.56±0.12	229.1± 0.8
1330	65	0.132±0.009	46.72 ±0.09	1292 ± 2	26.81±0.08	196.4± 0.6
1560	65	0.955±0.014	7.936±0.050	525.8± 0.8	30.66±0.58	223.0± 4.0
Integrated		3.437±0.075	1668 ±8	52654 ±72	30.95±0.16	225.0± 1.1
Sample: Grubenberg 02						$J = 4.095*10^{-3}$
770	45	0.364±0.030	46.42 ±0.05	1478 ± 3	29.50±0.20	205.8± 1.3
860	65	0.248±0.034	156.9 ±0.4	5134 ±12	32.25±0.13	223.8± 0.8
940	65	0.161±0.001	144.4 ±0.4	4771 ±10	32.70±0.11	226.7± 0.7
980	65	0.160±0.087	212.0 ±0.5	6909 ±52	32.35±0.29	224.5± 1.9
1030	65	0.151±0.055	146.8 ±0.4	4872 ±11	32.88±0.16	227.9± 1.1
1070	65	0.192±0.018	77.76 ±0.10	2594 ± 6	32.61±0.11	226.2± 0.7
1140	65	0.213±0.052	121.0 ±0.2	4005 ±11	32.57±0.16	225.9± 1.1
1170	65	0.211±0.024	104.7 ±0.1	3513 ± 7	32.94±0.10	228.3± 0.7
1230	65	0.241±0.026	276.3 ±0.7	9061 ±47	32.52±0.19	225.6± 1.3
1300	65	0.281±0.001	84.91 ±0.15	2902 ± 6	33.19±0.09	229.4± 0.6
1380	65	0.337±0.037	5.102±0.036	252.2± 0.6	29.90±2.13	208.4±14.0
1550	65	0.925±0.033	5.206±0.040	455.0± 1.1	34.83±1.92	240.6±12.4
Integrated		3.483±0.139	1381 ±7	45936 ±75	32.50±0.18	225.4± 1.2
Sample: Raidelberg 01						$J = 1.143*10^{-3}$
500	60	0.082±0.002	1.198±0.060	119.9± 0.2	80.0±4.1	157.9± 7.7
600	60	0.046±0.059	2.632±0.078	279.3± 0.6	100.9±6.3	197.0±11.5
700	60	0.278±0.014	5.794±0.158	685.4± 1.1	104.1±2.9	202.9± 5.4
750	60	0.051±0.019	9.656±0.190	1077 ± 4	109.9±2.3	213.6± 4.2
800	60	0.035±0.020	10.61 ±0.21	1191 ± 1	111.3±2.2	216.2± 4.1
850	60	0.082±0.002	11.25 ±0.17	1273 ± 3	111.0±1.7	215.6± 3.2
900	60	0.029±0.014	11.42 ±0.27	1325 ± 1	115.2±2.8	223.3± 5.1
950	60	0.093±0.012	19.28 ±0.10	2269 ± 3	113.1±0.6	219.4± 1.1
1000	60	0.067±0.008	29.89 ±0.07	3415 ± 6	113.6±0.4	220.3± 0.7
1080	60	0.109±0.015	32.07 ±0.09	3671 ± 4	113.4±0.4	220.1± 0.7
1140	60	0.411±0.059	42.98 ±0.09	4964 ± 6	112.7±0.5	218.6± 0.9
1200	60	0.109±0.025	32.14 ±0.07	3671 ± 4	113.2±0.4	219.6± 0.7
1260	60	0.148±0.047	16.56 ±0.09	1911 ± 3	112.7±1.0	218.7± 1.9
1350	60	0.224±0.022	12.87 ±0.06	1516 ± 2	112.7±0.8	218.7± 1.4
1500	60	0.146±0.020	1.848±0.068	243.7± 0.5	108.5±5.1	211.1± 9.4
Integrated		1.908±0.105	240.7 ±1.5	27612 ±13	112.3±0.7	218.0± 1.3
Sample: Raidelberg 02						$J = 9.20*10^{-4}$
530	45	0.471±0.015	13.00 ±0.05	1491 ± 5	104.0± 0.7	164.9± 1.0
610	40	0.555±0.008	26.90 ±0.09	3670 ± 8	130.3± 0.6	204.3± 0.8
650	40	0.370±0.019	36.45 ±0.13	5189 ±38	139.4± 1.2	217.7± 1.7
690	40	0.618±0.007	33.18 ±0.14	4839 ±11	140.3± 0.7	219.1± 1.0
720	45	0.351±0.012	20.96 ±0.15	3057 ± 7	140.9± 1.1	219.9± 1.6
740	45	0.381±0.011	18.47 ±0.15	2735 ± 7	141.9± 1.2	221.5± 1.8
770	45	0.497±0.018	28.11 ±0.10	4063 ± 9	139.3± 0.6	217.6± 0.9
830	45	0.318±0.009	2.168±0.048	402.4± 1.0	142.1± 3.4	221.7± 5.1
880	45	0.369±0.017	0.650±0.058	178.1± 0.4	105.9±12.4	167.8±18.7
920	45	0.408±0.029	0.562±0.048	167.6± 0.4	83.5±16.8	133.6±26.0
1400	45	1.228±0.021	0.820±0.062	445.9± 1.1	100.9±11.0	160.1±16.6
1500	50	1.445±0.021	0.388±0.046	444.7± 1.3	44.6±17.0	72.5±27.1
Integrated		7.013±0.058	181.7 ±1.3	26682 ±43	135.5± 1.0	211.9± 1.4
Sample: Schlitzloch 01						$J = 4.272*10^{-3}$
770	45	0.469±0.011	6.782±0.056	280.7± 1.0	20.91±0.53	154.4± 3.7
870	65	0.396±0.039	57.89 ±0.33	1728 ± 3	27.81±0.26	202.5± 1.8
940	65	0.263±0.030	81.01 ±0.23	2503 ± 9	29.93±0.18	217.1± 1.2
960	65	0.308±0.041	143.3 ±0.4	4491 ±12	30.69±0.15	222.3± 1.0
970	65	0.210±0.025	90.20 ±0.26	2856 ± 7	30.96±0.14	224.1± 1.0
1020	65	0.231±0.002	102.3 ±0.2	3201 ± 8	30.61±0.10	221.8± 0.6
1070	65	0.239±0.035	161.0 ±0.5	4994 ±12	30.56±0.14	221.4± 0.9
1100	65	0.296±0.039	132.9 ±0.5	4185 ±14	30.83±0.18	223.2± 1.2
1140	65	0.156±0.036	16.69 ±0.13	572.7± 2.7	31.52±0.71	227.9± 4.8
1280	65	0.080±0.001	5.842±0.058	217.2± 0.4	33.10±0.33	238.6± 2.2
1500	60	1.762±0.066	5.530±0.066	700.2± 2.5	32.38±3.62	233.8±24.2
Integrated		4.412±0.115	803.4 ±4.8	25729 ±26	30.39±0.19	220.2± 1.3
Sample: Schlitzloch 02						$J = 4.210*10^{-3}$
770	45	0.967±0.018	14.35 ±0.06	571.9± 2.0	19.92±0.41	145.3± 2.9
870	65	0.701±0.022	115.7 ±0.3	3550 ± 7	28.87±0.12	206.9± 0.8
940	65	0.404±0.015	139.8 ±0.6	4326 ±10	30.08±0.15	215.1± 1.0
960	65	0.407±0.023	173.5 ±0.5	5355 ±11	30.16±0.11	215.6± 0.7
970	65	0.241±0.017	94.24 ±0.16	2926 ± 6	30.28±0.10	216.4± 0.7
1020	65	0.316±0.014	173.7 ±0.5	5321 ± 9	30.07±0.10	215.0± 0.7
1070	65	0.609±0.009	287.2 ±0.6	8780 ±45	29.93±0.17	214.1± 1.1
1100	65	0.450±0.006	137.3 ±0.4	4333 ±11	30.57±0.12	218.4± 0.8
1140	65	0.035±0.032	26.61 ±0.10	852.4± 2.1	31.64±0.38	225.6± 2.6
1220	75	0.673±0.039	16.86 ±0.07	716.5± 2.3	30.69±0.70	219.2± 4.7
1500	80	1.636±0.019	6.006±0.054	675.2± 2.2	31.87±1.07	227.1± 7.2
Integrated		6.439±0.071	1185 ±7	37406 ±51	29.94±0.18	214.1± 1.2

The corresponding irradiation parameters (J-values) are listed in the headings.

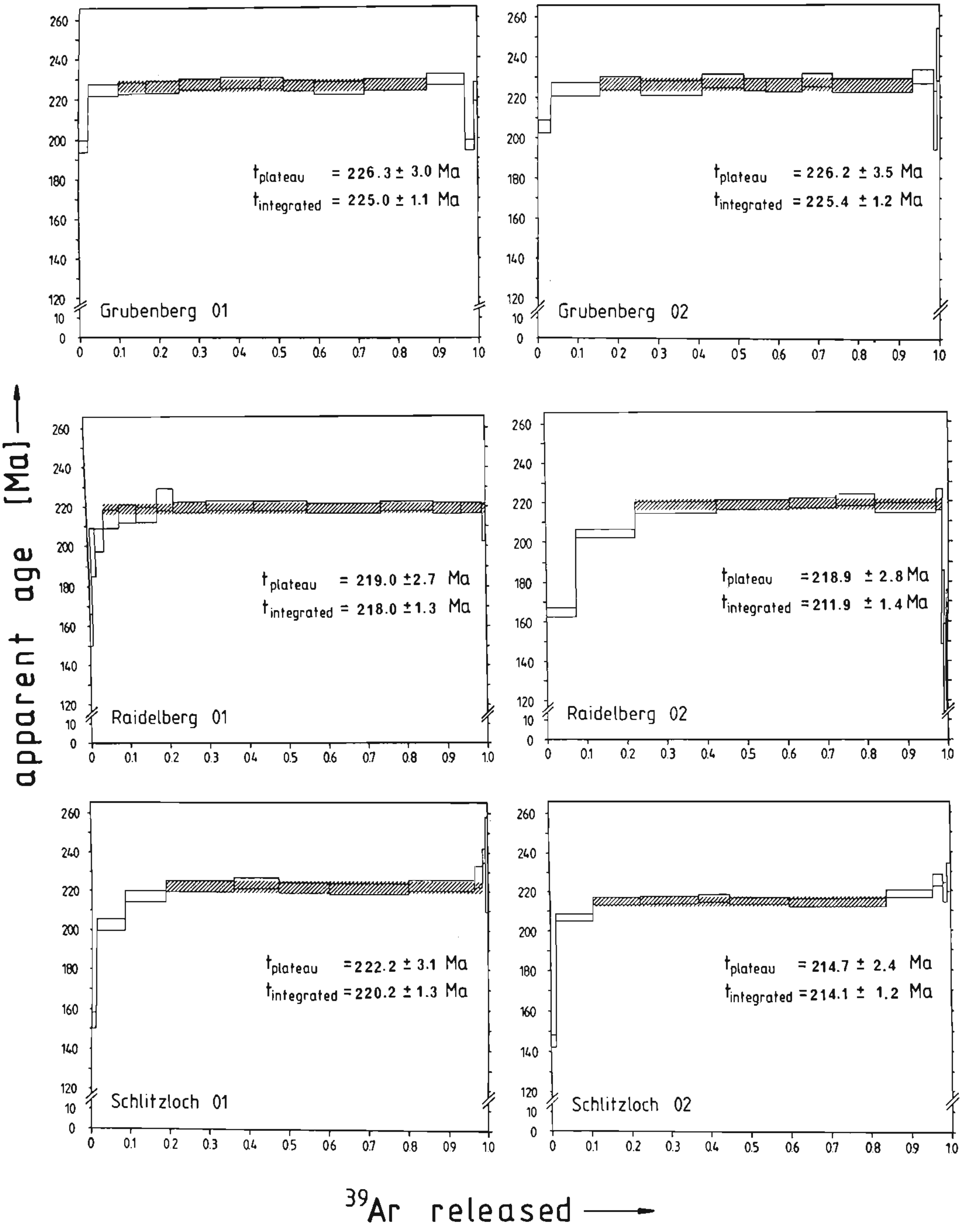

Fig. 7. $^{40}Ar/^{39}Ar$ degassing spectra of neogenic K-feldspars (adularia) from the Walhausen mineralizations. The hatchings within the spectra indicate the plateau areas.

micro veins. This overprint may account for a disturbance of the isotopic system. Thus, a slight lowering of the crystallization age from about 219-225 Ma, corresponding to the age of sample Schlitzloch 01, to about 215 Ma, may be assumed for sample Schlitzloch 02. The disturbance postulated cannot be recognized by a significant difference in the shape of the $^{40}Ar/^{39}Ar$ degassing spectrum compared with that of the undisturbed adularia systems. The slightly younger Rb/Sr age of the sample Grubenberg 03, in contrast to the $^{40}Ar/^{39}Ar$ ages of the samples Grubenberg 01 and 02 also may possibly be due to disturbances by ore impregnations of the K-feldspars in the Rb/Sr separate.

On the whole, two hydrothermal events at about 224 Ma and about 219 Ma could be established by the adularia measurements for the mineralizations of the Walhausen area. The geological significance of the isotopic data is evidenced by age concordances of the Rb/Sr and K/Ar systems, petrographically different types of adularia, and geographically different locations.

7. Geological discussion

The dated events of hydrothermal activity correspond to the ages Carnian to Norian (Keuper), *i.e.*, Upper Triassic (Odin and Létolle, 1982). Mineralizing events in the Saar-Nahe region during the Upper Triassic also have been confirmed by $^{40}Ar/^{39}Ar$ measurements on hydrothermally formed celadonite from the vein mineralization "Louise", which are in concordance with U+Th/He ages of haematite from this mineralization (Bähr *et al.*, 1987). There is a hiatus of approximately 70 Ma between the intrusion of the host rocks at about 290 Ma and the hydrothermal activities at Walhausen. Therefore, a derivation of the ore-forming solutions from the volcanic rocks in the sense of a post-magmatic hydrothermal succession is unlikely. This is also supported by the $^{87}Sr/^{86}Sr$ ratios on calcites of the mineralizations with a variation of 0.7103 ± 0.0006. In case of a primary magmatic source, the Sr ratios of the gangues should about agree approximately with the initial value of the magmatic rock. However, the initial Sr values of the "Grenzlager" magmatic rocks are 0.706, measured on apatites from rhyolites and tuffs (Lippolt and Raczek, 1979) and on clinopyroxene from basalt (Göpel and Zindler, 1980), which is significantly lower than the Sr ratios of the calcites. The Sr values of the location Schlitzloch vary in a distinct range from about 0.7097 to 0.7100. The Sr ratios of the location Grubenberg are significantly higher, ranging from 0.7107 and 0.7109. This indicates differentiations of the hydrothermal solutions on a local scale, which is also supported by the age difference between the adularia from the locations Grubenberg and Raidelberg. Similar conclusions for other hydrothermal vein deposits were made by Norman and Landis (1983) and Mertz (1987) based on systematic investigations of Sr isotopic characteristics of paragenetic successions.

In previous studies (*e.g.* Schneiderhöhn, 1941 ; Geis, 1959) it was assumed that the mineralizations in the Saar-Nahe region are post-magmatic formations derived from the Permian volcanism in this area. As the experimental data indicate, however, this may not be applied to the Walhausen mineralizations. According to the paragenetic sequence worked out by Müller (1983 ; 1988) for the Saar-Nahe region, and the time mark for this sequence supplied by the adularia data, the majority of the mineralizations from this region are not temporally related to the intrusion of the Permian magmatic rocks. Most likely, there is a subordinate hydrothermal phase derived from the volcanic rocks. $^{40}Ar/^{39}Ar$ measurements on hydrothermal celadonite from the Saar-Nahe region (Kastel mineralization) yielded an integrated age of about 270 Ma (Mertz, 1987) which may be evidence for such a phase.

Sample Raidelberg 02 contains, besides adularia of type A, about 40 % metasomatically formed K-feldspar of type B. There is no age difference between it and sample Raidelberg 01 which is composed exclusively of adularia of type A. Such a result indicates that both the K-feldspar types A and B were formed at the same time and in the same genetic context. Petrography and isotopic data suggest K-metasomatism initiated by a hydrothermal phase. This event obviously provided a favorable environment for processes of mobilization, enrichment and deposition of metal.

The experimental proof of two distinct mineralizing events with a hiatus of about 5 Ma indicates multi-stage hydrothermal activities on a local scale during geological periods of times. The multi-stage characteristic of solution-transport processes is also clearly reflected in the zoned structure of the adularia (*cf.* Fig. 6). The results of U/Pb datings on U ores of the vein deposit Höhenstein/Oberpfalz, FRG (Carl *et al.*, 1985), on adularia from mineralizations of the Lizard District/SW England (Halliday and

Mitchell, 1976) or on authigenic illites and sericites of the Clara vein mineralization/ Schwarzwald, FRG (Bonhomme *et al.*, 1983 ; Lippolt *et al.*, 1986) tendentiously confirm this assertion.

Halliday and Mitchell (1984) compiled isotopic age data measured on hydrothermal K-feldspars and clay minerals from mineralizations from Southern and Western Europe. As a result, a pronounced peak of mineralizing activity at 220 Ma was identified, which is in very good agreement with the adularia ages presented here. Halliday and Mitchell (1984) proposed that this 220 Ma event "was related to an initial rapid fracturing of the crust associated with the break up of Pangaea, which was related with an increase in the geothermal gradient and penetration of the crust by surface waters which returned via fissure systems". Such a model, applied to the Walhausen veins, plausibly provides a super-regional geotectonic framework for these mineralizations. Sufficient indication of deep-going syn-Triassic tectonic activities are found in the area of the so-called Eifeler North-South zone (*e.g.* Echle and Gusonne, 1985), a geotectonic unit, that contains the Walhausen mineralizations in its southern part.

8. Conclusions

Within the mineralizations investigated, adularia (Or contents > 98 mol.%, relatively high degree of Al,Si disorder) are found as co-genetic compounds in the hydrothermal succession.

The age concordances of independant isotopic clocks, petrographically differing adularia types and geographically different mineralizations confirm the undisturbed condition of the isotopic system of the K-feldspars.

Deteriorations of the Ar retention of adularia may be caused by syn- or post-genetic hydrothermal overprinting (*e.g.* ore impregnations).

Hydrothermal activities associated with K-metasomatic processes took place in the area of the Walhausen mineralizations at about 224 Ma and 219 Ma (Upper Triassic).

The hiatus of 5 Ma between both hydrothermal events indicates multi-stage mineralizing activities on a local scale during geological periods of time.

The majority of the epigenetic mineralizations in the Saar-Nahe region have been deposited in the syn- or post-Upper Triassic. The genesis of these mineralizations is not related to the Permian magmatism of this area.

This is also supported by the $^{87}Sr/^{86}Sr$ variation of 0.7103 ± 0.0006 on paragenetic calcites, which is markedly higher than the initial values of the magmatic host rocks.

The established mineralizing events confirm the existence of a super-regional hydrothermal phase in Europe during the Upper Triassic.

Acknowledgement : Prof. E. Eberhard (Hannover) and Prof. G. Frenzel (Heidelberg) kindly offered facilities to carry out X-ray structural and microprobe analyses. Neutron irradiation was performed by the staff of the Nuclear Research Centre, Jülich (FRG). This study received financial support through grants ("Erzdatierungen", "Adular-Isotopenalter") from the German Research Community (DFG), Bonn. R. Wernicke improved the English version of this paper by valuable lingual suggestions.

References

Alexander, E.C. Jr., Mickelson, G.M. and Lanphere, M.A. (1978) : MMhb-1 : A new Ar40-Ar39 dating standard. Short pap. 4th Int. Conf. Geochron. Cosmochron. Iso. Geol., Geol. Survey open-file rep. 78-701, 6-8.

Badham, J.P.N. (1975) : Mineralogy, paragenesis and origin of the Ag-Ni, Co arsenide mineralization, Camsell River, N.W.T., Canada. *Mineral. Deposita*, **10**, 153-175.

Bambauer, H.U. (1960) : Der permische Vulkanismus in der Nahemulde. *N. Jb. Min.*, **Abh. 95**, 141-199.

Bass, M.N. and Ferrara, G. (1969) : Age of adularia and metamorphism, Quachita Mountains, Arkansas. *Am. J. Sci.*, **267**, 491-498.

Bähr, R., Mertz, D.F. and Lippolt, H.J. (1987) : The reliability of U-Th/He ages of kidney-type hematite. *Terra cognita*, **7**, 2-3, 229.

Bonhomme, M.G., Bühmann, D. and Besnus, Y. (1983) : Reliability of K-Ar dating of clays and silifications associated with vein mineralizations in Western Europe. *Geol. Rundsch.*, **72**, 105-117.

Brockamp, O. and Zuther, M. (1985) : K/Ar-Datierungen zur Alterseinstufung lagerstättenbildender Prozesse. *Naturwiss.*, **72**, 141-143.

Buchanan, L.J. (1981) : Precious metal deposits associated with volcanic environments in the southwest. *Ariz. Geol. Soc. Dig.*, **14**, 237-262.

Carl, C., Dill. H., Kreuzer, H. and Wendt, I.

(1985) : U/Pb- und K/Ar-Datierungen des Uranvorkommens Höhenstein/Oberpfalz. *Geol. Rundsch.*, **74**, 483-504.

Dreyer, G., Franke, W.R., Stapf, K.R.G. and contributions of other authors (1983) : Geologische Karte des Saar-Nahe-Berglandes und seiner Randgebiete 1:100 000, Institut für Geowissenschaften der Johannes-Gutenberg-Universität Mainz.

Echle, W. and Gusonne, R. (1985) : Das Trias-Dreieck der Nordeifel und seine Erzvorkommen. *Fortschr. Miner.*, **63**, 2, 25-38.

Falke, H. (1959) : Neue Erkenntnisse über die Grenzlagergruppe des Saar-Nahe-Rotliegenden. *Geol. Rundsch.*, **48**, 66-76.

Franke, W. and Ghobarkar, H. (1982) : The morphology of hydrothermally grown K-feldspar. *N. Jb. Min.*, **Mh. 2**, 57-68.

Geis, H.-P. (1959) : Minerallagerstätten der Saar-Nahe-Senke. *Geol. Rundsch.*, **48**, 83-91.

Goldsmith, J.R. and Laves, F. (1954a) : The microcline-sanidine stability relations. *Geochim. Cosmochim. Acta*, **5**, 1-19.

—, — (1954b) : Potassium feldspars structurally intermediate between microcline and sanidine. *Geochim. Cosmochim. Acta*, **6**, 100-118.

Göpel, C. and Zindler, A. (1980) : Nd- und Sr-Isotopiedaten von basaltischen Gesteinen der Saar-Nahe-Senke. *Fortschr. Miner.*, **58**, 1, 37-38.

Halliday, A.N. and Mitchell, J.G. (1976) : Structural, K-Ar and Ar^{40}/Ar^{39} age studies of adularia K-feldspars from the Lizard Complex, England. *Earth Planet. Sci. Let.*, **29**, 227-237.

—, — (1984) : K-Ar ages of clay-size concentrates from the mineralization of the Pedroches Batholith, Spain, and evidence for Mesozoic hydrothermal activity associated with the break up of Pangaea. *Earth Planet. Sci. Let.*, **68**, 229-239.

Hess, J.C. (1985) : Petrogenese und tektonische Stellung jungphanerozoischer Magmatite des Großen Kaukasus. Dissertation, 176 p., Heidelberg.

Hess, J.C. and Lippolt, H.J. (1986) : $^{40}Ar/^{39}Ar$ ages of tonstein and tuff sanidines : new calibration points for the improvement of the Upper Carboniferous time scale. *Chemical Geology* (Isotope Geosc. Sec.), **59**, 143-154.

Hintze, C. (1897) : Handbuch der Mineralogie, Bd. II, 2. Hälfte, 1736 p., von Veit (Leipzig).

Joseph, D., Bellon, H., Derre, C. and Touray, J.-C. (1973) : Fluorite veins dated in the 200 million year range at La Petite Verrière and Chavaniac, France. *Econ. Geol.*, **68**, 707-708.

Jung, D. (1970) : Permische Vulkanite im SW-Teil des Saar-Nahe-Pfalz-Gebietes. *Aufschl. Sonderbd.*, **19**, 185-201.

Kastner, M. and Siever, R. (1979) : Low temperature feldspars in sedimentary rocks. *Am. J. Sci.*, **279**, 435-479.

Kämpf, H. and Pilot, J. (1981) : Zur Altersbestimmung hydrothermaler Fluorit-Paradoxit-Quartz-Mineralisationen des SW-Vogtlandes mit Hilfe der K-Ar-Methode. *Freiberger Forschungsh.*, **C 360**, 119-132.

Lippolt, H.J. and Hess, J.C. (1983) : Isotopic evidence for the stratigraphic position of the Saar-Nahe Rotliegend volcanism I. $^{40}Ar/^{40}K$ and $^{40}Ar/^{39}Ar$ investigations. *N. Jb. Geol. Paläont.*, **Mh. 12**, 713-730.

Lippolt, H.J., Hess, J.C., Raczek, I. and Venzlaff, V. (1989) : Isotopic evidence for the stratigraphic position of the Saar-Nahe Rotliegend volcanism II. Rb-Sr investigation. *N. Jb. Geol. Paläont.*, **Mh.**, (in press).

Lippolt, H.J., Mertz, D.F. and Huck, K.-H. (1986) : The genesis of the Clara and Friedrich-Christian vein deposits/Central Schwarzwald (FRG) : Evidence from Rb-Sr, Sr^{87}/Sr^{86}, K-Ar and Ar^{40}/Ar^{39} investigations. *Terra cognita*, **6**, 2, 228.

Lippolt, H.J., Mertz, D.F. and Ziehr, H. (1985) : The Late Permian Rb-Sr age of a K-Feldspar from the Wölsendorf mineralization (Oberpfalz, FR Germany). *N. Jb. Miner.*, **Mh. 2**, 49-57.

Lippolt, H.J. and Raczek, I. (1979) : Isotopische Altersbestimmungen an vulkanischen Biotiten des Sarr-Nahe-Perms. *Fortschr. Miner.*, **57**, 1, 87.

MacKenzie, W.S. (1954) : The orthoclase-microcline inversion. *Miner. Mag.*, **30**, 354-366.

Mensing, T.M. and Faure, G. (1983) : Identification and age of neoformed paleozoic feldspar (adularia) in a Precambrian basement core from Scioto County, Ohio, USA. *Contrib. Miner. Petrol.*, **82**, 327-333.

Mertz, D.F. (1987) : Isotopengeochemische und mineralogische Untersuchungen an postvariscischen hydrothermalen Silikaten. Dissertation, 207 p., Heidelberg.

Mertz, D.F., Lippolt, H.J. and Eberhard, E. (1989b) : ^{39}Ar diffusion and $^{40}Ar/^{39}Ar$ dating of adularia. *Terra abstracts*, **1**, 353.

Mertz, D.F., Lippolt, H.J. and Schnorrer-Köhler, G. (1989a) : Early Cretaceous mineralizing activity in the St. Andreasberg ore district (SW Harz/FR Germany). *Mineral. Deposita*, **24**, 9-13.

Munhá, J., Fyfe, W.S. and Kerrich, R. (1980) : Adularia, the characteristic mineral of felsic spilites. *Contrib. Miner. Petrol.*, **75**, 15-19.

Müller, G. (1975) : Hydrothermaler K-Feldspat von Walhausen und Kastel (N-Saarland). *Bergb. Pfalz, Saarland, Lothringen, Miner.*, **9**, 83-88.

— (1983) : Mineralisationen im Raum Saar-Nahe-Pfalz (Paragenesen und Abfolgen). *Schriftenr. Gesellsch. Dt. Metallh.- u. Bergl.*, **41**, 115-126.

— (1988) : Gedanken zu den Mineralisationen im Saarland und in seiner Umgebung. *Aufschluss*, **39**, 5, 257-268.

Norman, D.I. and Landis, G.P. (1983) : Source of mineralizing components in hydrothermal ore fluids as evidenced by $^{87}Sr/^{86}Sr$ and stable isotope

data from the Pasto Bueno deposit, Peru. *Econ. Geol.*, **78**, 451-465.
Odin, G.S. and Létolle, R. (1982) : The Triassic time scale in 1981. *in* : "Numerical dating in stratigraphy", G.S. Odin, ed., Wiley & Sons (Chichester etc.), part I, 523-533.
Purdy, J.W. and Stalder, H.A. (1973) : K-Ar ages of fissure minerals from Swiss Alps. *Schweiz. Min. Petr. Mitt.*, **53**, 79-97.
Rich, R.A., Holland, H.D. and Petersen, U. (1977) : Hydrothermal uranium deposits. *Dev. Econ. Geol.*, **6**, 264 p.
Riederer, J. (1966) : Der Paradoxit von Wölsendorf. *N. Jb. Miner.*, **Mh.**, 131-142.
Rittmann, K.L. (1984) : Argon in Hornblende, Biotit und Muskovit bei der geologischen Abkühlung - $^{40}Ar/^{39}Ar$-Untersuchungen. Dissertation, 280 p., Heidelberg.
Rose, A. (1970) : Zonal relations of wall rock alteration and sulfide distribution at porphyry Cu deposits. *Econ. Geol.*, **65**, 920-936.
Schneiderhöhn, H. (1941) : Lehrbuch der Lagerstättenkunde. Die Lagerstätten der magmatischen Abfolge, Fischer (Jena), I. Bd., 858 p.
Silberman, M.L., Chesterman, C.W., Kleinhampl, F.J. and Gray, C.H.Jr. (1972) : K-Ar ages of volcanic rocks and gold-bearing quartz-adularia veins in the Bodie mining district, Mono County, California. *Econ. Geol.*, **67**, 597-604.
Silberman, M.L. and Ashley, R.P. (1970) : Age of ore deposition at Goldfield, Nevada, from K-Ar dating of alunite. *Econ. Geol.*, **65**, 352-354.
Staudacher, T., Jessberger, E.K., Dörflinger, D. and Kiko, J. (1978) : A refined ultrahigh-vacuum furnace for rare gas analysis. *J. Phys. E : Sci. Instrum.*, **11**, 781-789.
Steiger, R.H. and Jäger, E. (1977) : Subcommission on Geochronology : Convention on the use of decay constants in geo- and cosmochronology. *Earth Planet. Sci. Let.*, **36**, 359-362.
Steiner, A. (1968) : Clay minerals in hydrothermally altered rocks at Wairakai, New Zealand. *Clays and Clay Minerals*, **16**, 193-213.
— (1970) : Genesis of hydrothermal K-feldspar (adularia) in an active geothermal environment at Wairakai, New Zealand. *Miner. Mag.*, **37**, 916-922.
Ziehr, H. (1967) : Das Nabburg-Wölsendorfer Flußspatrevier. *Aufschl. Sonderbd.*, **16**, 215-253.

Received 24 February 1989
Accepted 2 October 1989

Veröffentlicht: Stuttgart 1990 März 2016 (www.geosaarmueller.de)